Coupled channel analysis of $\bar{p}p$ annihilation into $\pi^0\pi^0\pi^0$, $\pi^0\eta\eta$ and $\pi^0\pi^0\eta$

Crystal Barrel Collaboration

C. Amsler[o], D.S. Armstrong[a,1], C.A. Baker[e], B.M. Barnett[c], C.J. Batty[e], M. Benayoun[f], K. Beuchert[b], P. Birien[a], P. Blüm[h], R. Bossingham[a], K. Braune[ℓ], J. Brose[k,2], D.V. Bugg[i], T. Case[a], S.U. Chung[k,3], A.R. Cooper[i], O. Cramer[ℓ], K.M. Crowe[a], T. Degener[b], H.P. Dietz[ℓ], N. Djaoshvili[f], S. v. Dombrowski[o], M. Doser[f], W. Dünnweber[ℓ], D. Engelhardt[h], M. Englert[ℓ], M.A. Faessler[ℓ], C. Felix[ℓ], P. Giarritta[o], R. Hackmann[c], R.P. Haddock[j], F.H. Heinsius[a], M. Herz[c], N.P. Hessey[ℓ], P. Hidas[d], C. Holzhaussen[h], P. Illinger[ℓ], D. Jamnik[ℓ,4], H. Kalinowsky[c], B. Kalteyer[c], B. Kämmle[g], T. Kiel[h], J. Kisiel[f,5], E. Klempt[c], H. Koch[b], M. Kobel[f,6], C. Kolo[ℓ], M. Kunze[b], M. Lakata[a], R. Landua[f], J. Lüdemann[b], H. Matthäy[b], R. McCrady[m], J.P. Merlo[a], C.A. Meyer[m], L. Montanet[f], A. Noble[o,7], R. Ouared[f], F. Ould-Saada[o], K. Peters[b], C.N. Pinder[e], G. Pinter[d], S. Ravndal[b], C. Regenfus[ℓ], E. Schäfer[k,8], P. Schmidt[g], M. Schütrumpf[b], R. Seibert[g], S. Spanier[o,9], H. Stöck[b], C. Straßburger[c], U. Strohbusch[g], M. Suffert[n], U. Thoma[c], M. Tischhäuser[h], D. Urner[o], C. Völcker[ℓ], F. Walter[k], D. Walther[b], U. Wiedner[g], N. Winter[h], J. Zoll[f], B.S. Zou[i], Č. Zupančič[ℓ]

[a] University of California, LBL, Berkeley, CA 94720, USA
[b] Universität Bochum, D-44780 Bochum, FRG
[c] Institut für Strahlen- und Kernphysik der Universität Bonn, D-53115 Bonn, FRG
[d] Academy of Science, H-1525 Budapest, Hungary
[e] Rutherford Appleton Laboratory, Chilton, Didcot OX11 0QX, UK
[f] CERN, CH-1211 Genève, Switzerland
[g] Universität Hamburg, D-22761 Hamburg, FRG
[h] Universität Karlsruhe, D-76021 Karlsruhe, FRG
[i] Queen Mary and Westfield College, London E1 4NS, UK
[j] University of California, Los Angeles, CA 90024, USA
[k] Universität Mainz, D-55099 Mainz, FRG
[ℓ] Universität München, D-80333 München, FRG
[m] Carnegie Mellon University, Pittsburgh, PA 15213, USA
[n] Centre de Recherches Nucléaires, F-67037 Strasbourg, France
[o] Universität Zürich, CH-8057 Zürich, Switzerland

Abstract

We confirm the existence of the two $I^G(J^{PC}) = 0^+(0^{++})$ resonances $f_0(1370)$ and $f_0(1500)$ reported by us in earlier analyses. The analysis presented here couples the final states $\pi^0\pi^0\pi^0$, $\pi^0\pi^0\eta$ and $\pi^0\eta\eta$ of $\bar{p}p$ annihilation at rest. It is based on a 3×3 K-matrix. We find masses and widths of $M = (1390\pm30)$ MeV, $\Gamma = (380\pm80)$ MeV; and $M = (1500\pm10)$ MeV, $\Gamma = (154 \pm 30)$ MeV, respectively. The product branching ratios for the production and decay into $\pi^0\pi^0$ and $\eta\eta$ of the $f_0(1500)$ are $(1.27 \pm 0.33) \cdot 10^{-3}$ and $(0.60 \pm 0.17) \cdot 10^{-3}$, respectively.

In three recent letters we have reported the observation of two scalar isoscalar resonances around 1370 and 1500 MeV [1–3] produced in $\bar{p}p$ annihilation at rest and which decay into $\pi^0\pi^0$ and $\eta\eta$. The analysis of the $\pi^0\pi^0\eta$ final state of $\bar{p}p$ annihilation at rest [4] revealed a new isovector scalar resonance, the $a_0(1450)$.

In this letter we report the results of a coupled channel analysis of the final states $\pi^0\pi^0\pi^0$, $\pi^0\pi^0\eta$ and $\pi^0\eta\eta$ based on the data presented in Refs. [2–4] and the $\pi\pi$ scattering data of Refs. [5,6]. The method uses the extension of the K-matrix formalism to production processes described by Aitchison [7] which was already used in the single channel analyses of Refs. [2–4]. This gives unitarity conserving amplitudes and allows to determine the coupling constants of the new resonances to $\pi^0\pi^0$ and $\eta\eta$ from a common fit. A simultaneous analysis of a lower statistical sample of these reactions using a N/D inspired method is given in [8].

The apparatus [9] and the reduction of data on $\bar{p}p$ annihilation into 6 photons has been discussed e.g. in Ref. [4]. After data reduction we found 712,000 $\pi^0\pi^0\pi^0$, 280,000 $\pi^0\pi^0\eta$ and 198,000 $\pi^0\eta\eta$ events. In order to improve the statistics for the $\pi^0\eta\eta$ channel we have set up a special trigger enhancing the fraction of events in this channel. The acceptance of the three final states is nearly uniform over the whole phase space with deviations of not more than about

---

[1] Now at William & Mary College, Williamsburg, USA.
[2] Now at Universität Dresden, Dresden, Germany.
[3] Now at BNL, Upton, New York, USA.
[4] University of Ljubljana, Ljubljana, Slovenia.
[5] University of Silesia, Katowice, Poland.
[6] Now at Universität Freiburg, Freiburg, Germany.
[7] Now at CRPP, Ottawa, Canada.
[8] Now at Max Planck Institute, München, Germany.
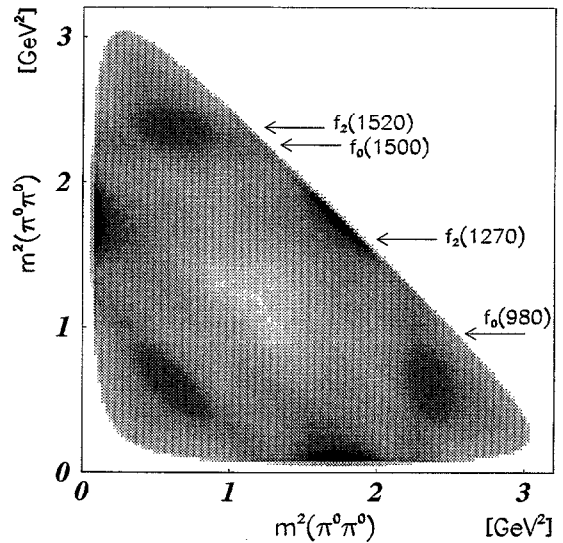[9] This work is part of the Ph.D. thesis of S. Spanier.

Fig. 1. The Dalitz plot of the $\pi^0\pi^0\pi^0$ final state. Each event is entered six times for symmetry reasons.

2%. Taking into account the detection and reconstruction efficiencies and the mesonic partial decay widths into two photons [16], we derived the annihilation branching fractions:

$$\begin{aligned} \mathrm{BF}(\bar{p}p \to \pi^0\pi^0\pi^0) &= (6.2 \pm 1.0) \cdot 10^{-3}, \\ \mathrm{BF}(\bar{p}p \to \pi^0\pi^0\eta) &= (6.7 \pm 1.2) \cdot 10^{-3}, \\ \mathrm{BF}(\bar{p}p \to \pi^0\eta\eta) &= (2.0 \pm 0.4) \cdot 10^{-3}. \end{aligned} \tag{1}$$

We now briefly recall the main features of the $\pi^0\pi^0\pi^0$, $\pi^0\pi^0\eta$ and $\pi^0\eta\eta$ Dalitz plots. The $3\pi^0$ Dalitz plot (Fig. 1) shows a strong contribution from $\bar{p}p \to f_2(1270)\pi^0$ with a decay angular distribution peaked in the forward and backward directions. This is characteristic for a spin-2 particle produced from the $^1S_0$ state of the $\bar{p}p$ atom. In the three corners, a clear homogeneously populated band, due to the new scalar meson $f_0(1500)$, and a blob are observed. The

Fig. 2. The Dalitz plot of the $\pi^0\eta\eta$ final state. Each event is entered twice for symmetry reasons.
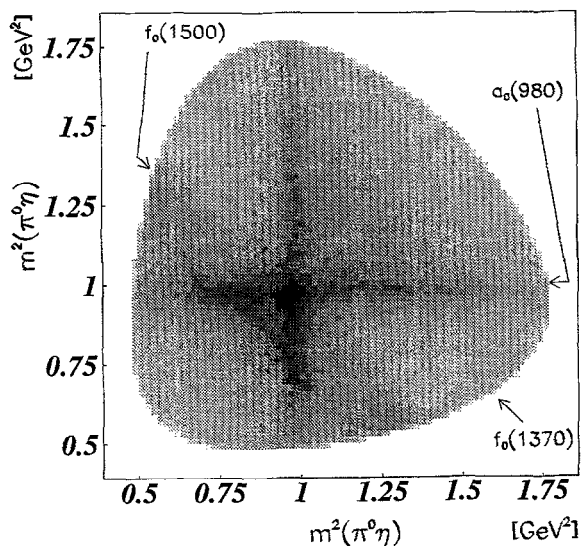

Fig. 3. The Dalitz plot of the $\pi^0\pi^0\eta$ final state. Each event is entered twice for symmetry reasons.

latter can be explained partly by interfering reflections from the low-energy $\pi^0\pi^0$ interaction, partly by a tensor resonance at 1520 MeV [1,2]. The mass and width of the $f_0(1500)$ were determined to be $M = (1500 \pm 15)$ MeV and $\Gamma = (120 \pm 25)$ MeV, respectively. Finally we notice a faint dip around 1 GeV evidencing production of the $f_0(980)$. This feature requires the introduction of a coupling to the $K\bar{K}$ channel. The $3\pi^0$ data can be described using $^1S_0$ as initial state only [2](see also [1]); the inclusion of atomic P states, however, improved the fit and led to a contribution of 30–50 % P-wave [2].

In the $\pi^0\eta\eta$ Dalitz plot (Fig. 2) one observes an accumulation of events in the center, originating from the triple interference of two $a_0(980)$ and an $\eta\eta$ band at about 1500 MeV. Additional intensity is also observed as an $\eta\eta$ band at a mass of (1360 ± 35) MeV, which we call $f_0(1370)$. The structure at 1500 MeV required the introduction of both a 0^{++} and a 2^{++} wave resonating at (1505 ± 15) MeV and (1530 ± 15) MeV, respectively. The scalar resonance has a width of (120 ± 30) MeV while the width of the tensor resonance is rather uncertain. For the $\pi^0\eta\eta$ Dalitz plot a good fit was obtained assuming pure S-wave annihilation [3].

The $\pi^0\pi^0\eta$ Dalitz plot (Fig. 3) exhibits clear evidence for the $a_0(980)$, the $f_0(980)$ and the $a_2(1320)$. These intermediate states interfere strongly with each
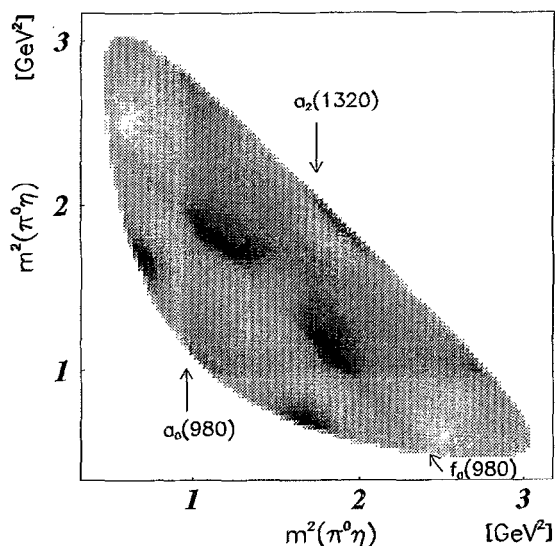
other, indicating the dominance of a single initial state $^1S_0$. Beside the $f_0(980)$ a resonance at a mass of 1330 MeV was required in the $\pi\pi$ S-wave. A satisfactory description of this annihilation channel can only be achieved with the introduction of a new isovector scalar resonance $a_0(1450)$ [4] with a mass of $(M = 1450\pm40)$ MeV and a width of $\Gamma = (270\pm40)$ MeV.

We now turn to the amplitudes for the coupled channel analysis. The partial wave analysis of the Dalitz plots was carried out using the K-matrix formalism in an extension to production processes which we call the P-vector approach [10]. We shall use the same method consistently to describe the three Dalitz plots simultaneously. The transition amplitudes are constructed as

$$A_{J^{PC}}(\mathbf{p}, \mathbf{q}) = \sum Z_{J^{PC},L,l}(\mathbf{p}, \mathbf{q}) \, F^l(\mathbf{q}) \, B^L(\mathbf{p}). \qquad (2)$$

The initial $\bar{p}p$ state is characterized by the quantum numbers J^{PC}, the final state by the quantum numbers L, l (L = angular momentum between the isobar and the recoil meson of momenta $\pm\mathbf{p}$; l = angular momentum of the isobar splitting into two mesons of momenta $\pm\mathbf{q}$).

The angular distribution is described by spin–parity functions $Z_{J^{PC},L,l}(\mathbf{p}, \mathbf{q})$ as given by Zemach [11]. The dynamical functions F^l consist of the product of a propagator $(I - iK\rho)^{-1}$ with a production vector P

[10]. We suppress the index l and obtain the vector

$$F = (I - iK\rho)^{-1}P. \tag{3}$$

In these formulae, I is the identity matrix and ρ the two-body phase space ($\rho = 2q/m$, q the decay momentum). The production vector P is given by a sum over resonance poles (with summation index α) produced with complex strengths β_α:

$$P_i = \sum_\alpha \frac{\beta_\alpha \, g_{\alpha i} B_i^l}{m_\alpha^2 - m^2}. \tag{4}$$

The B_i^l represent centrifugal barrier factors [12]. The resonances couple to the different final states i with couplings $g_{\alpha i}$:

$$g_{\alpha i} = \sqrt{\frac{m_\alpha \Gamma_{\alpha i}}{\rho_i(m_\alpha)}}. \tag{5}$$

The $\Gamma_{\alpha i}$ are the partial widths of pole α into the final state i.

In the coupled channel analysis one can be more restrictive concerning the production strengths β_α. The production of a resonance in combination with a spectator particle is controlled by the β_α while its decay into two body channels is described by the partial widths. A resonance seen in different final states in combination with the same spectator particle corresponds to the same production mechanism: therefore, the β_α are equal. The creation of a resonance recoiling against different spectators does not set such a constraint. As an example of different productions consider the $f_0(980)$ which is observed as a peak in $\pi^0\pi^0\eta$ (η recoiling) and as a dip in $\pi^0\pi^0\pi^0$ (π^0 recoiling).

The coupling of different channels is achieved by an appropriate choice of a K-matrix

$$K_{ij}(m) = \sum_\alpha \frac{g_{\alpha i} g_{\alpha j} B_i^l B_j^l}{m_\alpha^2 - m^2} + c_{ij} \tag{6}$$

with c_{ij} being real constants which are only relevant for the $\pi\pi$ S-wave. We guarantee that the $\pi\pi$ S-wave scattering amplitude goes to zero near threshold by multiplying the K-matrix (Eq. (6)) with a factor $(m^2 - 2m_\pi^2)/m^2$. The K-matrix is related to the relativistic invariant scattering amplitude T, which has the same propagator as the production amplitude F, by

$$T = (I - iK\rho)^{-1}K. \tag{7}$$

The amplitude $\rho_1 T_{11}$ is applied to the $\pi\pi$ scattering data on phase shift and inelasticity [5,6].

Note that the K-matrix poles are not the physical pole positions (Breit-Wigner poles). Those are obtained from the reaction amplitude in the complex energy plane. The introduction of a coupling to the $K\bar{K}$ channel is motivated by the behaviour of $\pi\eta$ and $\pi\pi$ at the $K\bar{K}$ threshold. Since no data on $K\bar{K}$ were included in this analysis, the width $\Gamma_{\bar{K}K}$ parameterizes the inelasticity to unconsidered open channels.

Let us now discuss the parametrization of the partial wave amplitudes in the coupled channel analysis. The pole positions obtained for the $\pi\pi$ and $\eta\eta$ S-waves from the analysis of each individual annihilation channel $3\pi^0$, $\pi^0\eta\eta$ and $\pi^0\pi^0\eta$ are compatible [2–4]. This fact leads us to assume that we have observed two resonances ($f_0(1370)$ and $f_0(1500)$), both decaying to $\pi\pi$ and $\eta\eta$. The low energy part of the $\pi\pi$ S-wave, which is accessible in $3\pi^0$, $\pi^0\pi^0\eta$ and the scattering data, in addition needs a K-matrix pole below $K\bar{K}$ threshold and one pole which parameterizes the steady increase of the $\pi\pi$ phase shift. A common description of the data sets therefore enforces the introduction of four-poles in the K-matrix. Since coupling to the $K\bar{K}$ channel is essential for the $\pi\pi$ S-wave, we have to use a 3×3 K-matrix with $\pi\pi$, $K\bar{K}$ and $\eta\eta$ as channel 1,2 and 3, respectively. The K-matrix in Eq. (6) can be rewritten as:

$$K_\alpha = \frac{1}{m_\alpha^2 - m^2} \begin{pmatrix} g_{\pi\pi}^2 & g_{\pi\pi}g_{\bar{K}K} & g_{\pi\pi}g_{\eta\eta} \\ g_{\bar{K}K}g_{\pi\pi} & g_{\bar{K}K}^2 & g_{\bar{K}K}g_{\eta\eta} \\ g_{\eta\eta}g_{\pi\pi} & g_{\eta\eta}g_{\bar{K}K} & g_{\eta\eta}^2 \end{pmatrix}_\alpha \tag{8}$$

with $K = \sum_\alpha K_\alpha + (c_{ij})$. For S-wave ($l = 0$) the centrifugal barrier factors B_i^l are equal 1. The g_i, which depend on α, are the coupling strengths of poles m_α in Eq. (5). Since we find new resonances in the mass range above 1.2 GeV, we use the scattering data [5,6] only for $\pi\pi$ masses below this value.

The $\pi^0\eta$ S-wave exhibits a $K\bar{K}$ threshold effect, too. Hence, we combine the $\pi^0\eta$ and $K\bar{K}$ channels in a 2×2 K-matrix which is applied to $\pi^0\pi^0\eta$ and $\pi^0\eta\eta$. The reaction amplitude calculated from the K-matrix is the Flatté-formula [13]. Two K-matrix poles are found to be needed.

The $\pi^0\eta$ D-wave ($a_2(1320)$ and $a_2(1600)$) is taken from the analysis of $\pi^0\pi^0\eta$ [4].

The $\pi\pi$ D-wave ($f_2(1270)$ and $f_2(1520)$) is parameterized by a 2-pole one-channel K-matrix in order to preserve unitarity. For the $\eta\eta$ D-wave a 1×1 K-matrix is used. The expected contribution of the reaction $\bar{p}p \to \pi^0 f_2(1270)$, $f_2(1270) \to \eta\eta$ is less than 1%.

It is well known that annihilation in liquid hydrogen occurs preferentially from S-states of the protonium [14]. For the coupled channel fits with a 3×3 K-matrix we assume that annihilation takes place from the $^1S_0$ initial state of the $p\bar{p}$ atom; possible contributions from P-state annihilation are neglected. This reduces the number of parameters significantly.

Before fitting the amplitudes to the different data samples one has to take into account the correct normalization between the data sets. The meson partial decay widths are included in the reconstruction efficiencies, and the population in the $\pi^0\eta\eta$ Dalitz plot is scaled down by the trigger enhancement factor. This procedure does not affect the statistical errors but for the coupled channel partial wave analysis it ensures that the total number of events in one of the final states corresponds to its branching ratio (Eq. (1)). The intensity calculated from the total amplitude (Eq. (2)) is compared to the number of events in each Dalitz plot cell of the individual data sets by means of a χ^2. The χ^2 minimization used the MINUIT [15] program package of CERN.

Notice that the fit is more restricted in comparison to the fits made earlier on each single annihilation channel and makes a common description of four different data samples. In this respect our parametrization gives a reasonable description of the data. The χ^2 contributions per data point of the $\pi^0\pi^0\pi^0$ ($\pi^0\pi^0\eta$, $\pi^0\eta\eta$) Dalitz plot are $\chi^2/N_{data} = 2448/1338$ ($2657/1738$, $2896/1798$). The total number of parameters is 34.

In Fig. 4 we demonstrate the fit quality by comparing the $\pi^0\pi^0$ mass distribution from $3\pi^0$ data with the fit result. In Fig. 5 we compare the $\pi^0\eta$ and $\eta\eta$ mass projections from the $\pi^0\eta\eta$ data with the fit results. The fit quality achieved for the $\pi^0\pi^0\eta$ Dalitz plot is similar to the one obtained in [4]. When data and fit results are compared to the Dalitz plots, no systematic deviations are observed. The description of the $\pi\pi$ scattering data yields $\chi^2/N_{data} = 46/39$ (see Fig. 6) for the mass range below 1200 MeV.
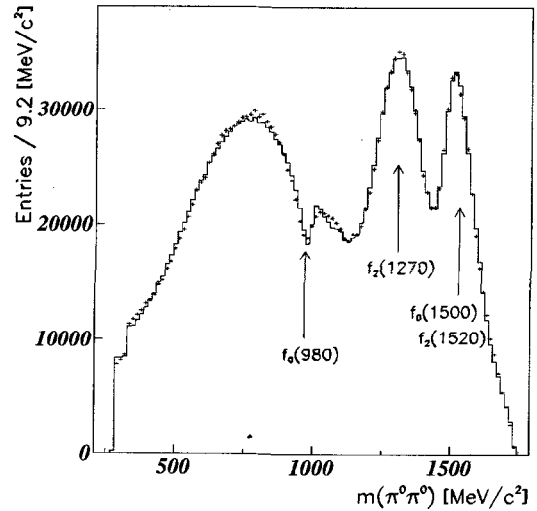

Fig. 4. The $\pi^0\pi^0$ mass projection of the $3\pi^0$ Dalitz plot. Crosses are data and the fit is superimposed. In the histogram, resonance mass positions are marked. Due to the symmetry of the final state their contributions appear at different places.

As a result of the coupled fit the $\pi^0\eta$ S-wave ($a_0(980)$ and $a_0(1450)$) and the D-wave ($a_2(1320)$ and $a_2(1600)$) remain compatible to the results obtained in the individual analyses of $\pi^0\pi^0\eta$ and $\pi^0\eta\eta$ [4,3]: The $a_0(1450)$ mass and width are $M = (1470 \pm 25)$ MeV and $\Gamma = (265 \pm 30)$ MeV, respectively. The corresponding parameters for $a_2(1320)$ are $M = (1315 \pm 5)$ MeV and $\Gamma = (112 \pm 5)$ MeV. Its contribution to the $\pi^0\eta\eta$ final state is below 1%. In the $\pi^0\pi^0\eta$ Dalitz plot a fraction of less than 2% non-resonant $\pi^0\eta$ P-wave is present.

The coupled fit reveals that the $\pi\pi$ D-wave requires two poles corresponding in the T-matrix to poles with masses and widths of $M = 1268$ MeV, $\Gamma = 180$ MeV and $M = 1552$ MeV, $\Gamma = 142$ MeV, respectively. Mass and width of the $f_2(1270)$ found in this analysis are in good agreement with the PDG-values [16]. The pole position of the higher-mass resonance agrees with the one obtained in the ASTERIX experiment [17]. The contributions of these two resonances to the $3\pi^0$ Dalitz plot are (13.9 ± 4.2)% for the $f_2(1270)$ and (9.6 ± 2.9)% for the higher mass pole. We caution the reader that the $f_2(1565)$ observed in [17] was produced from P-states of the $p\bar{p}$ atom in $\bar{p}p$-annihilation in hydrogen gas. As mentioned, we do not allow for P-state annihilation, and therefore our rates for the state
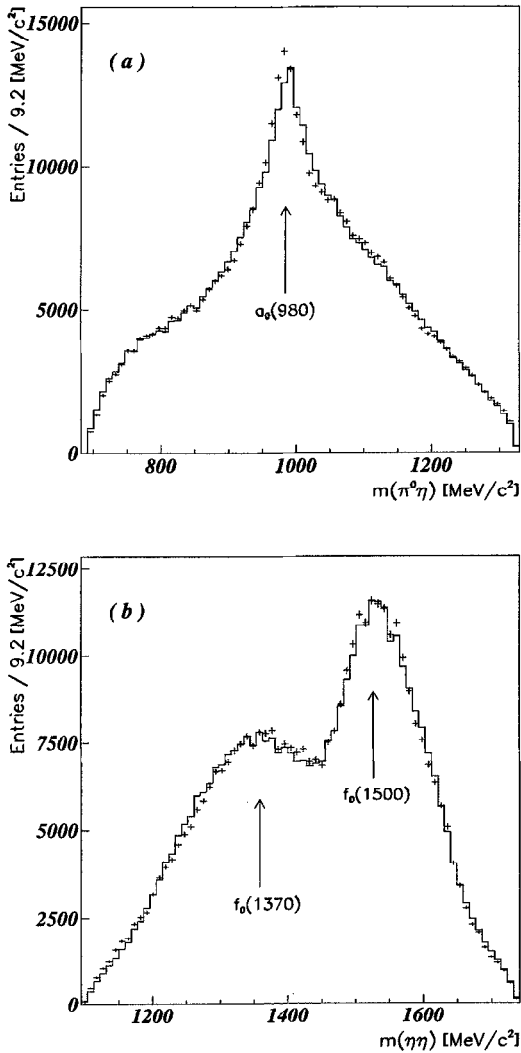
Fig. 5. $\pi^0\eta$ (a) and the $\eta\eta$ (b) mass distributions of the $\pi^0\eta\eta$ Dalitz plot, fit and data shown together. Prominent scalar resonance features are marked.

Fig. 6. Scattering data [5,6] and the fit result in the $\pi\pi$ mass range up to 1200 MeV.

Table 1
S-wave T-matrix pole positions $(M - i\Gamma/2)$ (in MeV) in the three relevant Riemann sheets with sign convention from [19]

Riemann sheet sign	II $-++$	III $--+$	IV $---$
	$996 - i56$	$953 - i55$	$938 - i35$
	$400 - i500$	$1100 - i137$	$1112 - i144$
	$1371 - i121$	$1407 - i167$	$1389 - i190$
	$1508 - i80$	$1501 - i83$	$1499 - i77$

at 1552 MeV may not be compared to the ASTERIX rates.

In the $\eta\eta$ D-wave we find one physical pole at $M = 1515$ MeV, $\Gamma = 328$ MeV. The contribution of the $\eta\eta$ D-wave is $(4.3 \pm 1.6)\%$ of $\pi^0\eta\eta$ and it may account for more than one tensor object, including in particular the $f_2'(1525)$. Assuming that the 2^{++} intensity can be assigned to $f_2'(1525)$, the product branching ratio $BR\{\bar{p}p \rightarrow f_2'; f_2' \rightarrow \eta\eta\} = (0.9 \pm 0.4) \cdot 10^{-4}$ is compatible with the upper limit of $1.3 \cdot 10^{-4}$ one
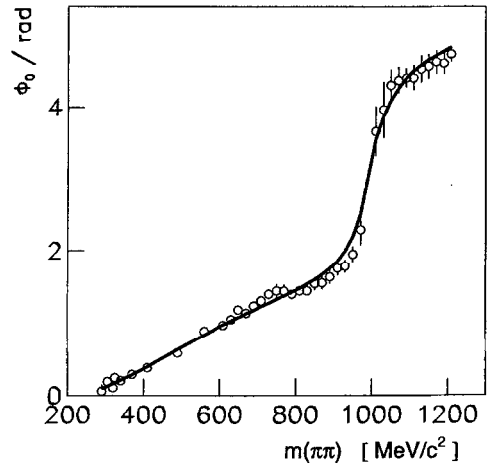
can predict from the non-observation in $\bar{p}p$ annihilation data [23], so far, and the decay branching ratio $f_2'(1525) \rightarrow \eta\eta$ given in [16]. The fact that $\pi\pi$ and $\eta\eta$ D-wave seem to resonate at different masses and widths could originate from neglecting atomic P-states. It might also indicate that the D-wave parameterizes a feature of annihilation dynamics (like nucleon exchange contributions [18]) which is not yet properly understood.

In a three-channel problem, resonances show up as poles in three of the eight different Riemann sheets of the complex energy plane. We follow the definitions of the Riemann sheets described in Ref. [19]. In the isoscalar S-wave we find the pole positions listed in Table 1.

The pole positions of the $f_0(980)$ from sheet II and sheet III may be compared to those found by Morgan and Pennington in a comprehensive discussion of the nature of this state [20]. From various fits they de-

duced poles at $((988 \pm 10) - i(24 \pm 6))$ MeV on sheet II and $(978 - i28)$ MeV on sheet III (no errors were given for the sheet III pole position). The fact that two nearby poles were observed was used to argue that the $f_0(980)$ is not a $K\bar{K}$ molecule. The masses found by us are close to their result; our width is, however, much broader. One can see the discrepancy to the scattering data in Fig. 6, where the fit does not reproduce exactly the increase of the scattering phase in the $f_0(980)$ region. The production data demand the larger width.

There is a second pole with a position found at 1100 MeV which is connected to the very broad pole at 400 MeV in sheet II; we identify this pole tentatively with the very wide 'background' resonance $f_0(1000)$ suggested in [20]. One may associate the pole with the scalar isoscalar ground state predicted in [21] to have mass and width of 1090 MeV and 850 MeV respectively. But for a Breit–Wigner resonance we should expect the pole position not to vary too much in the different Riemann sheets. We find that the position does move steadily from 1100 MeV to 400 MeV, the value found in sheet II, when we vary the sign of the coupling of the resonance to $K\bar{K}$. This behaviour prevents a straightforward interpretation of the pole as $q\bar{q}$ state. In sheet II, a width of 1000 MeV is found; so this pole parameterizes the attractive low-energy $\pi\pi$ interaction.

The pole positions of mesons with masses above the $\eta\eta$ threshold should be extracted from sheet IV (for which the path to the physical region is closest). We find the following masses and widths of the two scalar $I = 0$ resonances

$$M = (1390 \pm 30) \text{ MeV}; \quad \Gamma = (380 \pm 80) \text{ MeV}$$

$$M = (1500 \pm 10) \text{ MeV}; \quad \Gamma = (154 \pm 30) \text{ MeV}. \tag{9}$$

The errors of masses and widths correspond to the spread in repeated fits with different representations of the production data and different weightnings of the data-samples.

We estimate the fraction of events assigned to the $f_0(1500)$ by squaring the amplitudes. Strictly speaking, branching ratios are not defined when interfering resonances lead to the same final state. The consistency of the sum of individual contributions with the total contribution is encouraging. We assign a fractional error of 20%. Thus we find branching ratios of

Table 2
Product branching ratios

BR($\bar{p}p \to$ PS X; X $\to$ PS PS)	$\times 10^{-3}$
$\bar{p}p \to \pi^0 f_0(980, 1370); f_0 \to \pi^0\pi^0$	3.48 ± 0.89
$\bar{p}p \to \pi^0 f_0(980, 1370); f_0 \to \eta\eta$	1.03 ± 0.29
$\bar{p}p \to \eta f_0(980, 1370); f_0 \to \pi^0\pi^0$	3.33 ± 0.65
$\bar{p}p \to \pi^0 f_0(1500); f_0(1500) \to \pi^0\pi^0$	1.27 ± 0.33
$\bar{p}p \to \pi^0 f_0(1500); f_0(1500) \to \eta\eta$	0.60 ± 0.17
$\bar{p}p \to \pi^0 f_2(1270); f_2(1270) \to \pi^0\pi^0$	0.86 ± 0.30
$\bar{p}p \to \pi^0 f_2(1520); f_2(1520) \to \pi^0\pi^0$	0.60 ± 0.20
$\bar{p}p \to \pi^0 a_0(980); a_0(980) \to \pi^0\eta$	0.81 ± 0.20
$\bar{p}p \to \eta a_0(980); a_0(980) \to \pi^0\eta$	0.19 ± 0.06
$\bar{p}p \to \pi^0 a_0(1450); a_0(1450) \to \pi^0\eta$	0.29 ± 0.11
$\bar{p}p \to \pi^0 a_2(1320); a_2(1320) \to \pi^0\eta$	2.05 ± 0.40

$$BR\{\bar{p}p \to \pi^0 f_0(1500); f_0(1500) \to \pi^0\pi^0\} = (1.27 \pm 0.33) \cdot 10^{-3}$$
$$BR\{\bar{p}p \to \pi^0 f_0(1500); f_0(1500) \to \eta\eta\} = (0.60 \pm 0.17) \cdot 10^{-3} . \tag{10}$$

The values are compatible with the studies of the individual data samples [2,3].

In the same way the branching ratios for the other resonances were determined and are listed in Table 2. The low energy part of the $\pi\pi$ S-wave cannot be separated into the individual pole contributions. Therefore the ratio for the sum of $f_0(980)$, $f_0(1370)$ and the broad object at 1100 MeV is given.

From the branching ratios of the $f_0(1500)$ in Eq. (10) one can calculate the invariant couplings. To do so the branching ratios are divided by the phase space factors $|q_i|$. Identifying the scalar resonance observed close to the $\eta\eta'$ in the $\pi^0\eta\eta'$ final state [22] with the scalar resonance at 1505 MeV one obtains for the couplings relative to $\pi\pi$:

$$\pi\pi : \eta\eta : \eta\eta' = 3 : 0.70 \pm 0.27 : 1.00 \pm 0.46 \tag{11}$$

Here $\pi\pi$ includes the charged modes. Errors are calculated from the branching ratios. In addition the error of the relative $\eta\eta'$ coupling accounts for a variation of the $f_0(1500)$ pole within a 2σ mass interval in Ref. [22]. An upper limit of 0.36 for the relative $K\bar{K}$ coupling of $f_0(1500)$ can be derived from bubble chamber experiment [23].

This decay pattern makes it difficult to establish the $f_0(1500)$ as a $q\bar{q}$ meson [24]. A possible interpretation is the glueball groundstate which is expected at this mass from lattice gauge theory [25,26]. The coupling pattern is in contradiction to expectations of flavour democracy in glueball decays. However, the observed ratios can be reproduced in a model which assumes a small admixture of $q\bar{q}$ from the nearby $f_0(1370)$ in the glueball wave function [27,28].

Summarizing we confirm our observation of two scalar isoscalar resonances by applying consistently the K-matrix formalism. This underlines the observations of the resonances in the different final states of $\bar{p}p$ annihilations at rest. The close agreement to the analyses of the individual channels gives further confidence that two $I^G(J^{PC}) = 0^+(0^{++})$ resonances exist in a rather small mass interval.

Acknowledgements

References

[1] V. Anisovich et al. (Crystal Barrel Collaboration), Phys. Lett. B 323 (1994) 233

[2] C. Amsler et al. (Crystal Barrel Collaboration), Phys. Lett. B 342 (1995) 433

[3] C. Amsler et al. (Crystal Barrel Collaboration), submitted to Phys. Lett. B

[4] C. Amsler et al. (Crystal Barrel Collaboration), Phys. Lett. B 333 (1994) 277

[5] L. Rosselet et al., Phys. Rev. D 15(1977) 574

[6] G. Grayer et al., Nucl. Phys. B 75 (1974) 189

[7] I.J.R. Aitchison, Nucl. Phys. A 189 (1972) 417

[8] D.V. Bugg, V.V. Anisovich, A. Sarantsev, B.S. Zou, Phys. Rev. D 50 (1994) 4412

[9] E. Aker et al., Nucl. Instr. Methods A 321 (1992) 69

[10] S.U. Chung et al., Partial wave analysis in K-matrix formalism, accepted for publication in Ann. Phys.

[11] C. Zemach, Phys. Rev. B 140 (1965) 97, 109

[12] F. von Hippel and C. Quigg, Phys. Rev. 5 (1972)624

[13] S.M. Flatté, Phys. Lett. B 63 (1976) 224

[14] C. Amsler et al., Phys. Lett. B 297 (1992) 214

[15] F. James and M. Roos, CERN-DD Long write-up D506, CERN, 1987

[16] Particle Data Group, Phys. Rev. D 50 (1994) 1

[17] B. May et al. (Asterix collaboration), Zeitschrift für Physik C 46 (1990) 203

[18] A. Gregorian, presented at NAN93, Moscow

[19] W.R. Frazer and A.W. Hendry, Phys. Rev. B 134 (1964) 1307

[20] D. Morgan and M.R. Pennington, Phys. Rev. D 48 (1993) 1185

[21] S. Godfrey and N. Isgur, Phys. Rev. D 32 (1985) 189

[22] C. Amsler et al. (Crystal Barrel Collaboration), Phys. Lett. B 340 (1994) 259

[23] L. Gray et al., Phys. Rev. D 27 (1983) 307

[24] S. Spanier, Meson resonances in $\bar{N}N$ annihilation at rest, LEAP'94 conference, Bled

[25] C. Michael, M. Teper, Nucl. Phys. B 314 (1989) 347

[26] G.S. Bali et al., Phys. Lett. B 309 (1993) 378

[27] C. Amsler, Light quark and gluonium spectroscopy, 27th International Conference on High Energy Physics, Glasgow, 1994

[28] C. Amsler and F. Close, Evidence for a Scalar Glueball submitted to Phys. Lett. B